NanoImpact 2 (2016) 29–37

Contents lists available at ScienceDirect

NanoImpact

journal homepage: www.journals.elsevier.com/nanoimpact

Research paper

Zinc oxide nanoparticles trigger cardiorespiratory stress and reduce aerobic scope in the white sucker, *Catostomus commersonii*

Neal Ingraham Callaghan, Garett Joseph Patrick Allen, Tess Eliza Robart, Christopher Anthony Dieni, Tyson James MacCormack *

Department of Chemistry and Biochemistry, Mount Allison University, Sackville, NB, Canada

ARTICLE INFO

Article history:
Received 11 February 2016
Received in revised form 11 June 2016
Accepted 13 June 2016
Available online 15 June 2016

Keywords:
Nanotoxicology
Gill morphology
Acetylcholinesterase
Atropine
Metabolism

ABSTRACT

Acute exposure to commercially-relevant zinc oxide nanoparticles (nZnO) can alter heart function and induce a cellular stress response in gill tissue of the white sucker (*Catostomus commersonii*), a freshwater teleost fish. The current study aimed to identify potential mechanisms underlying the cardiorespiratory effects of nZnO exposure and to characterize the ecophysiological importance of nZnO toxicity. Gill morphology in white suckers exposed to nZnO was examined by scanning electron microscopy and indications of mild irritation were observed. Cardiorespiratory function was assessed using electrocardiography and opercular pressure fluctuations and the caudal artery was cannulated for injection of the acetylcholine receptor antagonist atropine to eliminate vagal influence on the heart. Exposure to nZnO had no significant effect on heart rate under the conditions tested, but ventilation rate rose ~30% in treated fish. Administration of atropine increased ventilation rate by 55% in control fish but had no effect in treated animals, indicating that nZnO alters parasympathetic control of respiration. Heart acetylcholinesterase activity decreased in nZnO-exposed fish, implying impaired acetylcholine metabolism may contribute to cardiorespiratory toxicity. Exposure to nZnO did not activate anaerobic metabolism, as we observed no changes in muscle lactate dehydrogenase kinetics or pH sensitivity. Decreases in both the maximum rate of oxygen consumption and aerobic scope indicate that exposure to nZnO reduces the aerobic capacity of the animal and suggests the observed toxicity has potential ecological importance. Overall, our findings suggest that nZnO-mediated damage to the gill epithelium alters cardiorespiratory regulation and subsequently impairs oxygen uptake and delivery.

1. Introduction

Nanoscale zinc oxide (nZnO) is a semiconductor and absorbs ultraviolet light, lending itself well to incorporation into electronics, solar panels, pigments in paints and cosmetics, sunscreens, and as a photocatalytic agent for detoxification and environmental remediation (Hao and Chen, 2012). Global nZnO production is estimated at 550 tons per year (Piccino et al., 2012), and its release into the environment (mainly in wastewater) exceeds 250 tons per year (Danovaro et al., 2008; Wong et al., 2010). Once in the environment, most nZnO is likely to precipitate due to its poor colloidal stability (Liu et al., 2014). In the sediment, nZnO is slow to degrade, lasting at least 14 days with no detectable changes to particle size (Gimbert et al., 2007). Bottom feeders such as the white sucker (*Catostomus commersonii*) used in this study can disturb the sediment potentially creating a localized zone of high nZnO concentration, making them of particular interest in toxicology studies. nZnO toxicity has been linked to two main mechanisms, oxidative stress and direct engineered nanomaterial (ENM)-protein interactions. The semiconductor nature of nZnO allows it to create reactive oxygen species (ROS) by passing electrons through structural defects to the local environment (Sharma et al., 2012; Xia et al., 2008). These ROS can then nonspecifically oxidize proteins and lipids, leading to loss of function and subsequent toxicity (Song et al., 2010). nZnO-induced lipid oxidation has been shown to reduce mitochondrial membrane potential, leading to mitochondrial dysfunction and the induction of apoptosis (Guo et al., 2013; Song et al., 2010; Xiong et al., 2011). Other studies have presented evidence that nZnO may directly interact with proteins to exert toxicity. Exposure to nZnO delayed hatch in zebrafish embryos by inhibiting the protease enzyme which weakens the chorion to facilitate hatching (Ong et al., 2014). Proteins can bind to ENMs, leading to protein denaturation and/or loss of function (Dieni et al., 2013; MacCormack et al., 2012).

We have previously shown induction of oxidative stress in white suckers from a relatively short exposure to nZnO (1.0 mg L^{-1} for 25 h; Dieni et al., 2014) and it triggers significant oxidative stress, developmental problems, and delayed hatch in zebrafish (Bai et al., 2010; Yu et al., 2011; Zhu et al., 2009, 2008). It is clear that aquatic nZnO exposure can induce biochemical indicators of toxicity in fish but evidence of the physiological importance of these responses is equivocal. Exposure to

* Corresponding author at: Department of Chemistry and Biochemistry, Mount Allison University, Sackville, NB E4L1G8, Canada.
E-mail address: tmaccormack@mta.ca (T.J. MacCormack).

http://dx.doi.org/10.1016/j.impact.2016.06.004
2452-0748/

silver ENMs sensitizes fish to hypoxia (Bilberg et al., 2010) and disrupts ion homeostasis (Schultz et al., 2012) but ionic silver is a well characterized toxin in freshwater fish and may contribute to such responses. White suckers acutely exposed to nZnO exhibited bradycardia and multiple indicators of gill damage but resting oxygen consumption rates (MO_2) did not change significantly (Bessemer et al., 2015), and there was little evidence of osmotic stress, suggesting only minor physiological consequences. To clarify the biological relevance of these responses, we quantified maximal O_2 consumption, aerobic scope, and sensitivity to hypoxia in fish acutely exposed to nZnO.

Gills have a large surface area with a high density of membrane proteins functioning in gas and ion exchange, excretion of nitrogenous wastes, and pH maintenance (Evans et al., 2005). A number of ENM formulations damage gill tissue (Federici et al., 2007; Smith et al., 2007) and previous work in our lab has suggested that nZnO exposure may impact gill chemoreceptor function (Bessemer et al., 2015). Teleost gills have independent, differentially innervated clusters of neuroepithelial cells (NECs) which act as chemoreceptors to detect either environmental or arterial O_2 partial pressures (PO_2). These receptors regulate heart (f_h) and ventilation (f_v) rates as part of the hypoxic response, and in most species f_h drops and f_v increases to maximize O_2 uptake and delivery when O_2 availability is limited (Milsom and Burleson, 2007; Perry and Desforges, 2006; Taylor et al., 2009). Hypoxia induces a depolarization of NECs, which is transmitted through the afferent and efferent vagus nerves to eventually release acetylcholine (ACh) at the sinoatrial node of the heart, lowering f_h (Milsom and Burleson, 2007; Regan et al., 2011). It is possible that ENM-induced gill damage could impact NEC function, causing a depression of f_h similar to a hypoxic bradycardia, as seen in white suckers (Bessemer et al., 2015). To investigate if this bradycardia is associated with changes in gill NEC induction of vagal signaling, we exposed fish to nZnO in the presence of atropine to block ACh receptors on the cardiac pacemaker. We also assessed the effects of nZnO exposure on acetylcholinesterase (AChE) activity in heart and gill to determine if reduced removal may lead to the accumulation of ACh and subsequent effects on f_h.

The hypoxic response in some freshwater teleosts is linked to gill remodeling and it is possible that some changes in the gills of fish exposed to nZnO are due to remodeling, rather than damage. When O_2 availability is not limiting, species like the crucian carp (*Carassius carassius*) exhibit an interlamellar cell mass (ILCM) that reduces gill surface area and minimizes the energetic costs of ion regulation (Sollid and Nilsson, 2006). Hypoxia leads to loss of the ILCM through apoptosis in order to increase surface area and improve O_2 uptake. If nZnO exposure stimulates gill NECs and triggers a pseudo hypoxic response in white suckers, the observed increase in heat shock protein expression, caspase activity, and NKA activity may be linked to gill remodeling (Bessemer et al., 2015). We investigated this possibility through electron microscopy analysis of gills collected from control and nZnO exposed fish.

The objectives of this study were two-fold; the first was to characterize the physiological impact of acute nZnO exposure on a model freshwater fish to determine if this common ENM significantly impacts whole-animal performance. Our second objective was to identify potential mechanisms underlying the changes in f_h and gill biochemistry previously observed in fish exposed to nZnO. We focused on a well-characterized, commercially-available nZnO formulation commonly included in consumer products and industrial applications.

2. Methods

2.1. Nanoparticles and characterization

Spherical, unfunctionalized nZnO were purchased from Nanostructured & Amorphous Materials Inc. (New Mexico, United States) and were a different batch of the same product used in our previous study (Bessemer et al., 2015). The particles had an advertised diameter of 25 nm and a zeta-potential (ζ) of +23.7 mV. Additional characterization was performed on this batch of nZnO to confirm the advertised specifications and the analyses previously carried out on this formulation in our laboratory (Bessemer et al., 2015; Dieni et al., 2014). Hydrodynamic diameter (144 nm) was assessed by dynamic light scattering with a Zetasizer Nano ZS (Malvern Instruments Ltd.; Worcestershire, United Kingdom) as done previously (Dieni et al., 2014). The ζ-potential was confirmed to be +21.1 mV, as in a previous study (Dieni et al., 2014), and was comparable to the curator's specifications. Scanning electron microscopy was used to confirm primary particle size as described previously (Dieni et al., 2014). Dissolution of this nZnO formulation was previously assessed via inductively coupled plasma mass spectrometry and release of free Zn^{2+} over 24 h was found to be below detection limits (0.05 mg L^{-1}; Bessemer et al., 2015). Given that studies were run in the same source water and that all other physicochemical characteristics of this nZnO batch were comparable, dissolution was not reassessed and is assumed to be negligible. In the absence of nZnO dissolution, a 'positive control' group exposed to free Zn^{2+} was deemed inappropriate.

Concentrated exposure stock solutions of 10 or 1.0 mg mL^{-1} (depending on the experiment) were prepared immediately before use by suspending dry nZnO powder in ddH_2O. The nZnO was dispersed by sonication (F60 Sonic dismembrator, Fisher Scientific, Waltham, MA) for 30–180 s, at full power.

2.2. Animal collection and holding

White suckers (*Catostomus commersonii*) weighing 245 ± 30 g were caught in Silver Lake (a freshwater lake naïve to industrial nZnO sources in Sackville, NB, Canada) by Fyke trap and immediately transported to the Harold Crabtree Aqualab at Mount Allison University. Fish were held in darkened 100 L tanks at 11 ± 1 °C. Water quality parameters, as previously presented (Bessemer et al., 2015) were: pH 7.46, 1240 μohm cm^{-1} conductivity, 660 mg L^{-1} total dissolved solids, and 323 mg L^{-1} hardness (as $CaCO_3$). Animals were fed to satiation daily with commercially-available sinking pellets (Corey Feed Mills Ltd., Fredericton, NB, Canada). Animals were acclimated at least 2 weeks prior to experimentation, and were not fed in the preceding 24 h. All experimentation was in accordance with guidelines established by the Canadian Council on Animal Care and protocols were approved by the Mount Allison University Animal Care Committee.

2.3. Experiment 1: effects on nZnO exposure on cardiorespiratory function

2.3.1. Surgical procedures

Fish were fitted with a PE-50 (Clay Adams Intramedic, Becton, Dickinson and Company, Franklin Lakes, NJ, USA) cannula in the caudal artery for pharmaceutical or sham injections. An incision c.a. 2.5 cm long was made just below the lateral line of the fish above the anal fin. The muscle tissue was gently teased apart using cotton swabs to expose the caudal artery. A vertical incision was then made in the caudal artery and the cannula inserted approximately 3 cm. The cannula contained heparinised, modified Cortland saline (in mmol L^{-1}: 120 NaCl, 0.88 $CaCl_2$, 0.90 $MgSO_4$, 3.35 KCl, 2.25 NaH_2PO_4, 5.00 $NaHCO_3$, 0.010 HEPES, 2.78 glucose, 4.00 sodium pyruvate, and 100 U mL^{-1} sodium heparin, pH 7.5). Hemorrhaging stopped immediately upon insertion of the cannula and proper placement was confirmed by withdrawing blood. The incision was closed with 4 sutures and the cannula anchored to the tail via a fourth suture placed approximately 0.5 cm posterior to the incision.

Heart rate was assessed using electrocardiography (ECG) as previously described (Bessemer et al., 2015). Briefly, fish were anaesthetized in buffered tricaine methanesulfonate (TMS) (150 mg L^{-1} TMS, 300 mg L^{-1} sodium bicarbonate) until unresponsive and then ram-ventilated with a maintenance TMS dose (75 mg L^{-1}, 150 mg L^{-1} sodium bicarbonate) for the course of the surgery. Two 10 mm subdermal F-E2 10 electrodes (Natus Neurology Incorporated - Grass Products,

Middleton, WI) were implanted under the surface of the skin along the pectoral girdle on either side of the heart and secured by a single suture. Ventilation frequency was measured using an MLT844 Physiological Pressure Transducer (ADInstruments, Colorado Springs, CO) attached to a section of PE-160 tubing. Approximately 3 cm of tubing was passed behind the operculum into the buccal cavity and secured by sutures. Both the ECG leads and the ventilation cannula were then secured to the body of the fish by an additional suture above the left-hand lateral line at the approximate midpoint, allowing the fish to swim unrestrained.

Fish were allowed to recover post-surgery in a modified 40 L cooler filled with 30 L continuously-aerated freshwater at 10 °C, with an aquarium pump to ensure sufficient mixing within the system. A length of ABS pipe, perforated to allow for water flow, was used to contain the fish and prevent tangling or displacement of cannulae or lead wires as previously described (Bessemer et al., 2015). Animals were left to recover overnight (15.5 h) before experiments were initiated. All animals were run individually in the same experimental system. Treatments were performed in a random order and the system was thoroughly cleaned between each run.

Regardless of treatment, animals were immediately sacrificed at the end of experimentation by an anaesthetic overdose in an 8 L freshwater bath containing 300 mg L^{-1} TMS, buffered with 600 mg L^{-1} sodium bicarbonate, until ventilation ceased. Fish were then killed by severing the spinal cord and tissue samples were collected, immediately flash-frozen in liquid nitrogen, and stored at −80 °C until use.

2.3.2. Experimental protocol

Following 15.5 h recovery, fish were treated with either nZnO or a sham addition of an equivalent volume of ddH_2O. For nZnO exposures, 30 mL of a 10 mg mL^{-1} stock solution was added directly to the water surrounding the animal to achieve a final nominal nZnO concentration of 10 mg L^{-1}. Experiment 1 focused on identifying mechanisms underlying nZnO bioactivity, therefore we did not attempt to replicate environmentally relevant exposure conditions. The chosen nZnO concentration is higher than the 1.0 mg L^{-1} dose used previously (Bessemer et al., 2015) to provide additional insight into potential dose-response effects. Five hours post-nZnO or sham treatment, fish were injected with either 1.2 mg kg^{-1} body mass atropine sulfate prepared in heparinized Cortland saline (as described above), or a saline only sham. The fish were then monitored for an additional 20 h before being sacrificed and tissues sampled, as described above. Each trial (N = 6 all treatments except N = 5 post-atropine nZnO) was comprised of a single fish in the tank. Samples of heart, brain, and liver tissue from selected animals in Experiment 1 were digested in nitric acid and analyzed for total zinc content using inductively coupled plasma mass spectrometry (ICP-MS, method reference EPA 200.8/EPA 200.7) by an accredited, independent laboratory (RPC Science & Engineering, Fredericton, NB, Canada).

2.4. Experiment 2: activation of anaerobic metabolism by nZnO exposure

Previous work suggested that nZnO exposure (1.0 mg L^{-1} for 25 h) initiated a pseudo hypoxic response in white suckers (Bessemer et al., 2015). Although exposure to nZnO did not impact glycogen stores or plasma lactate and glucose, it did significantly reduce aconitase activity, suggesting aerobic metabolism may be impaired (Dieni et al., 2014). To investigate this possibility, we characterized white muscle lactate dehydrogenase (LDH) kinetics in fish exposed to nZnO or control conditions. Randomly selected fish (N = 10 both treatments) were individually placed inside the modified cooler system containing 30 L of continuously circulated and aerated well water at 10 °C. Within the cooler, fish were placed inside a perforated 10 cm diameter ABS pipe to mimic the holding conditions utilized in the cardiorespiratory and respirometry studies (see below). Animals were allowed to acclimate overnight before being exposed to either 1.0 mg L^{-1} nZnO or a sham addition of ddH_2O. Exposures lasted 30 h before fish were euthanized by an anesthetic overdose and white muscle tissue sampled, flash frozen in liquid N_2 and stored at −80 °C.

2.5. Experiment 3: effects of nZnO exposure on physiological performance

2.5.1. Intermittent closed-loop respirometry

Intermittent closed-loop respirometry was employed to measure maximum O_2 consumption rate (MO_{2max}), resting oxygen consumption rate (MO_{2rest}), and critical O_2 tension (P_{crit}). A Q-BOX AQUA respirometry system (Qubit Systems, Kingston, ON) was housed inside a modified cooler containing 30 L air-saturated freshwater at 11 ± 1 °C as in our previous study (Bessemer et al., 2015). Oxygen consumption measurements were taken over 5 min with 10 min flushes with aerated water between measurements.

An exhaustive chase protocol was used to stimulate MO_{2max}. Multiple studies have shown this method to be as or more effective at stimulating MO_{2max} than critical swimming speed tests (Reidy et al., 1995; Soofiani and Priede, 1985). Single white suckers (N = 7 both treatments) were moved from their holding tank to a darkened, cylindrical chase tank containing 30 L air-saturated freshwater maintained at 11 ± 1 °C. Fish were then exposed to either 1.0 mg L^{-1} nZnO or a sham addition of an equivalent volume of ddH_2O for 15 h. After exposure, fish were chased by hand until they were no longer responsive (approx. 3–5 min) (Reidy et al., 1995). Animals were then immediately transferred into the respirometry system and MO_{2max} recorded, with nZnO present at 1.0 mg L^{-1} for treatment fish. Oxygen consumption was continually monitored for an additional 25 h to allow recovery from the chase protocol and determination of MO_{2rest}.

2.6. Analytical procedures

2.6.1. Acetylcholinesterase activity

AChE activity was assessed in samples of brain, heart ventricular muscle, and gill tissue (from the first arch) taken from white suckers in Experiment 1 (Section 2.3). AChE cleaves ACh into acetic acid and choline. AChE activity was quantified using a commercially available kit (ab128871, Abcam Inc., Toronto, ON) according to the manufacturer's instructions. Briefly, samples were thawed and immediately homogenized in assay buffer using a hand-held mini-homogenizer (Argos Technologies Pestle Mixer, Thomas Scientific, Swedesboro, NJ). Samples were then diluted appropriately and mixed into a reaction buffer containing ACh and 5.5′-dithiobis-(2-nitrobenzoic acid) (DTNB). Enzyme activity was measured at 410 nm by a Spectramax 190 microplate spectrophotometer (Molecular Devices, Sunnyvale, CA, USA) and SoftMax Pro software.

2.6.2. Lactate dehydrogenase kinetics

White muscle samples from animals in Experiment 2 were homogenized using a Polytron ®PT 10/35 GT (Kinematica Inc., Bohemia, NY) for 3 × 10 s at 1:5 (w:v) buffer containing (in mmol L^{-1}): Na_3PO_4 50, EDTA 5, EGTA 5, β-mercaptoethanol 10, β-glycerophosphate 30, phenylmethanesulfonyl fluoride 1, pH 7.2. Samples were then centrifuged at 10,000 ×*g* for 10 min at 4 °C. The resultant pellets were discarded, and the supernatants kept on ice. LDH activity assays were carried out in a 300 μL reaction at a final concentration of 50 mmol L^{-1} Na_3PO_4 (pH 7.2) containing 30 μL diluted supernatant. Maximum enzyme activity (V_{max}) was determined across a pH range of 6.20 to 8.20 using saturating substrate concentrations of 0.500 mM pyruvate and 1.60 mM NADH in the forward (pyruvate to lactate) direction, and 10.0 mM lactate and 1.00 mM NAD + in the reverse (lactate to pyruvate) direction. LDH activity was measured at 340 nm using a Spectramax 190 microplate spectrophotometer. The Michaelis constant (K_m) for each substrate was also assessed by holding one substrate at saturating concentration while varying the other from approximately 0.01–2× its saturating concentration. The resulting affinity curves

were fit with a Michaelis-Menten model to determine K_m. These assays were validated to ensure that the potential presence of nZnO did not cause bias in the assay methodology, as interactions between ENMs and enzymes or assay components may lead to data artefacts (MacCormack et al., 2012; Ong et al., 2014). nZnO was added to control supernatants at a final concentration of 1.0 mg L^{-1}. The V_{max} of LDH was then assessed between nZnO- and sham-treated supernatants to ensure nZnO had no direct effect on the assay's validity.

2.6.3. Gill scanning electron microscopy analysis

The upper portion of the second gill arches from fish in Experiment 3 were analyzed by SEM to determine if nZnO exposure led to epithelial remodeling or damage. Similar gill samples were also analyzed from 5 fish taken directly from the holding tanks to ensure the chase protocol did not influence gill morphology. Once excised from the animal, gill filaments were cut into portions of approximately 1 mm^2, washed 3 times with 100 mmol L^{-1} Na_3PO_4 buffer (pH 7.4), and fixed in 2.5% glutaraldehyde in the same buffer. Samples were then kept at 4 °C for up to 2 weeks before further processing. Samples were rinsed 4 times in Na_3PO_4 buffer, beginning at 4 °C and warming stepwise to room temperature. Samples were then dehydrated in stepwise ethanol solutions in water (20, 50, 70, 85, 95%) for 10 min at each step, followed by 4 × 10 min rinses in anhydrous ethanol. They were then critical point dried in liquid CO_2 using a DCP-1 critical point drying apparatus (Denton North America, Moorestown, NJ) and mounted on 32 mm aluminum specimen supports using colloidal graphite. Samples were sputter-coated with 20 nm Au using a Hummer 6.2 sputtering unit (Anatech USA, Union City, CA) with argon as the source gas. Samples were imaged with a JSM-5600 SEM (JOEL USA, Peabody, MA) operating at 10 kV and a 48 mm working distance. Occurrence frequency of apical pits of c.a. 0.5–2 μm diameter, mucous cells, and ionocytes of c.a. 4–8 μm width on the filament epithelium were noted in three representative zones of an image at a magnification of 500×, in randomized images to prevent viewer bias. To distinguish between cells, pavement or epithelial cells were identified by size and the presence of microridges and microbridges (Tano de la Hoz et al., 2014). Mucous cells were identified by size, concavity, and the presence of mucous globules (Tano de la Hoz et al., 2014). Mitochondria-rich cells or ionocytes were identified by concavity, size, surface texture, and confirmed by relative abundance (Dymowska et al., 2012; Tano de la Hoz et al., 2014). All histology was conducted blindly on randomized samples.

2.7. Data analysis and statistics

During experimentation, ECG signals were passed through a P55 AC pre-amplifier (Grass Products) which was grounded to a reference electrode placed in the tank water. Amplified ECG signals were collected on a PowerLab 8/26 data acquisition system (ADInstruments) and analyzed using default settings on LabChart 8 software equipped with an ECG analysis module. Signals from the pressure transducer attached to the ventilation cannula were passed through a bridge amplifier and data collected using the same PowerLab. The pressure transducer was calibrated to 0 and 20 cm H_2O using a static water column manometer. Heart and ventilation rates were determined manually on LabChart 8 by averaging the number of events over a 5 min interval each hour. Early-exposure data (pre-atropine injection) were analyzed by combining both no-atropine and atropine-injected groups by their respective control or nZnO treatments.

For Experiment 3, rates of O_2 consumption were determined each hour by linear regression of a representative 5 min O_2 trace and converted to MO_2 using functions in the LoggerPro software (Vernier Software and Technology, Beaverton, OR, USA). Rates were corrected for bacterial O_2 consumption in the system by running the system without a fish in the chamber. Aerobic scope was calculated as the difference between MO_{2max}, immediately following the chase protocol, and MO_{2rest} after the animal had recovered for 24 h.

All statistical analyses were completed using SPSS 21 (IBM Corporation, Armonk, NY). Data were tested for homogeneity of variance or sphericity, as appropriate. Heart rate and f_v changes pre- and post-atropine, AChE activity, individual aerobic metabolism parameters (MO_{2max}, MO_{2rest}, and aerobic scope), and LDH kinetic parameters (V_{max} and K_m) were compared by unpaired two-tailed *t*-test. Time course data on f_h and f_v, as well as MO_2 during the aerobic scope trial were analyzed by split-plot ANOVA. Gill SEM image cell occurrence frequencies were compared by unpaired two-tailed *t*-test. LDH V_{max} data over a pH range was normalized to the pH 7.2 value for each treatment and direction, and analyzed by split-plot ANOVA. In all statistical tests, significance was assigned at $p < 0.05$.

3. Results

3.1. Nanoparticle characterization

Fig. 1 shows an SEM image of the nZnO utilized in the study, confirming the advertised primary particle diameter of 25 nm. Dynamic light scattering analysis of an nZnO suspension indicated a hydrodynamic diameter of 144 nm and ζ-potential of +21.1 mV, comparable to the manufacturer's specifications of +23.7 mV.

3.2. Experiment 1: tissue zinc accumulation and cardiorespiratory impact of nZnO exposure

Brain, heart, and liver tissue from a subset of control and 10 mg L^{-1} nZnO-exposed fish (N = 3 for each treatment) were analyzed for total zinc content to investigate potential uptake of nZnO or accumulation of Zn^{2+} associated with nZnO degradation. There were no significant differences between total zinc content across treatment groups in any of the tissues examined. Total zinc content in brain (7.2 ± 0.6 vs 8.0 ± 0.1 μg g^{-1}), heart (19.6 ± 0.9 vs 19.0 ± 1.4 μg g^{-1}), and liver (36.8 ± 3.1 vs 35.0 ± 3.4 μg g^{-1}) were similar between control and nZnO-exposed fish, respectively, suggesting little to no uptake of nZnO or Zn^{2+} in these tissues under the acute exposure regime tested.

Fig. 2 illustrates findings from cardiorespiratory analysis of white suckers exposed to 10 mg L^{-1} nZnO in Experiment 1. In a previous study, exposure to 1.0 mg L^{-1} of the same nZnO formulation triggered

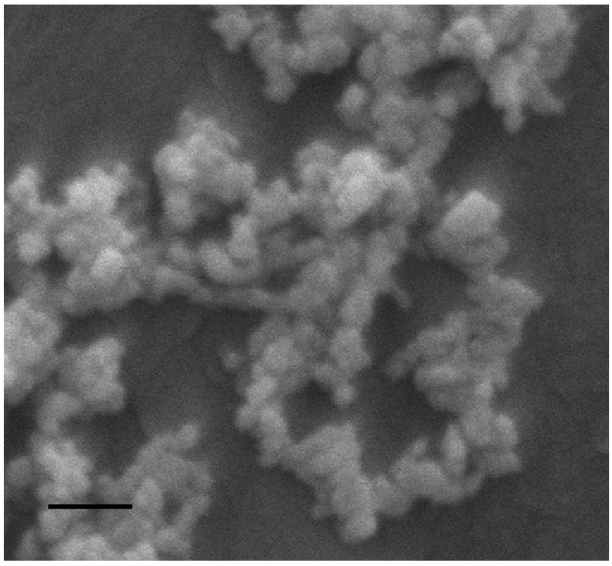

Fig. 1. Scanning electron micrograph of a dried nZnO suspension. The sample was coated with ca. 5 nm gold and images were collected using a JSM-5600 (JEOL USA, Inc., Peabody, MA) scanning electron microscrope at 10 kV and 8 mm working distance. Scale bar = 200 nm. (For interpretation of the references to colour in this figure legend, the reader is referred to the web version of this article.)

a significant decrease in f_h after 15 h (Bessemer et al., 2015). In the current study, f_h did not change with nZnO treatment at any point within the exposure period. Resting f_h prior to sham or nZnO treatment was higher than in our past study (~35 vs. 27 beats min^{-1}, respectively), likely due to the additional stress associated with the arterial cannulation procedure. In control fish, f_v tended to slow in the first 5 h following sham addition of ddH_2O. In contrast, f_v rose by ~30% over the same time frame in nZnO-treated fish, which was significantly different from the pattern in control animals ($p = 0.004$).

It is possible the additional stress of arterial cannulation masked subtle changes in parasympathetic control over f_h resulting from nZnO exposure. To address this possibility, a separate group of fish was injected with the muscarinic ACh receptor blocker atropine 5 h after the addition of nZnO or sham control. Injection of atropine increased f_h by ~50% in

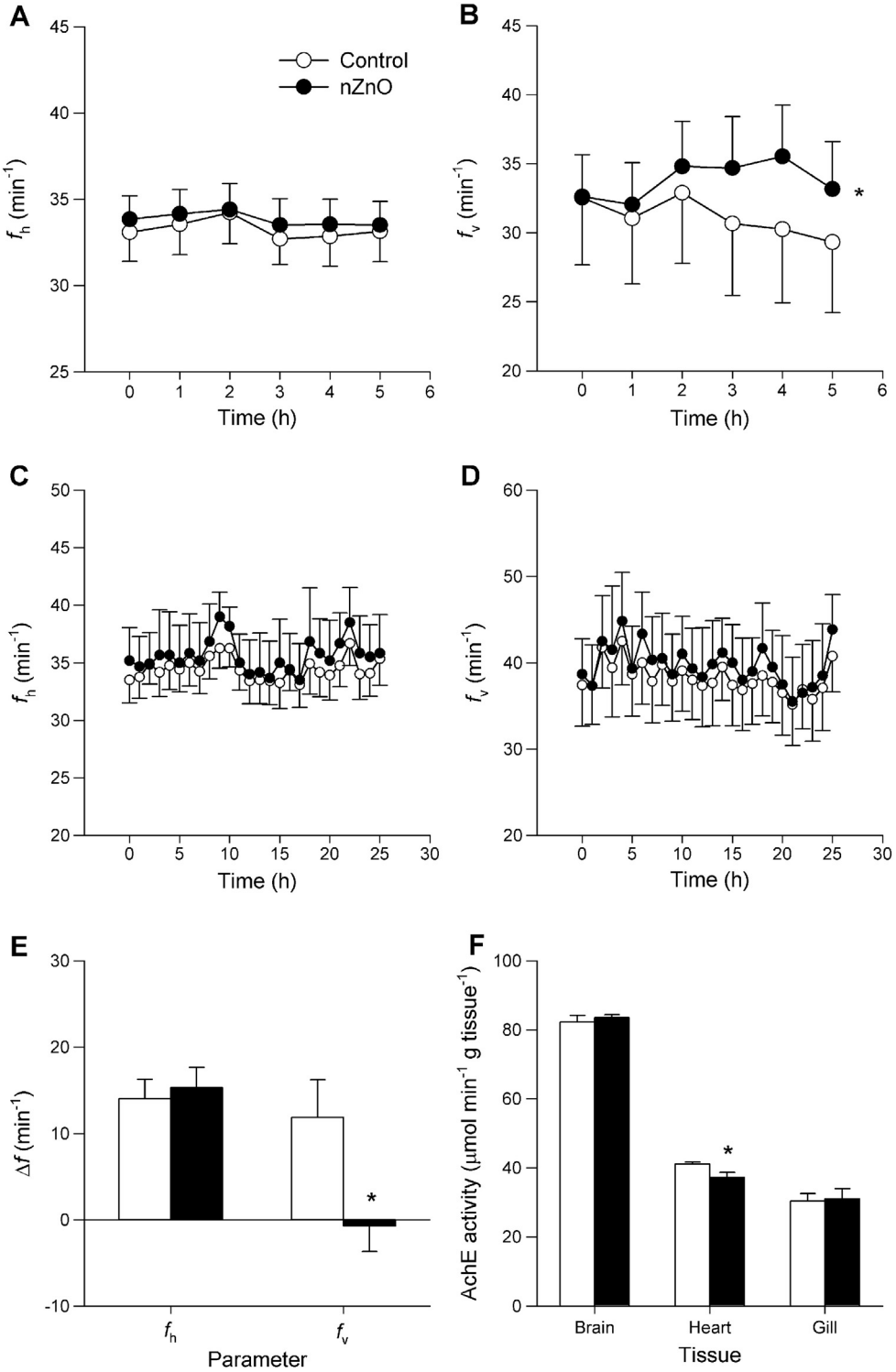

Fig. 2. A, heart (f_h) and B, ventilation (f_v) rates from white suckers from 0–5 h post-treatment with either a sham or 10 mg L^{-1} nZnO exposure (control N = 12, nZnO N = 11). C, f_h and D, f_v from white suckers post-treatment with either a sham or 10 mg L^{-1} nZnO exposure (N = 6, both treatments). Change in E, f_h and F, f_v 1 h post-atropine injection in white suckers treated with a sham or 10 mg L^{-1} nZnO exposure (control N = 6, nZnO N = 5). Data is presented as mean ± SEM. Asterisks denote a significant difference between treatments ($p < 0.05$).

Table 1
Kinetic parameters of white muscle lactate dehydrogenase from white suckers (N = 10 both treatments) exposed to a sham or 1 mg L^{-1} nZnO suspension, assayed at pH 7.2. Maximum reaction velocity (V_{max}) is expressed in nmol min^{-1} mg $protein^{-1}$ for forward (pyruvate-consuming) and reverse (pyruvate-producing) directions. Michaelis constants are expressed in μM, except for lactate which is expressed in mM. Data is presented as mean ± SEM. No significant difference was found between treatments within any parameter.

Treatment	V_{max}		Michaelis constant (K_m) (μmol L^{-1})			
	Forward	Reverse	Pyruvate	Lactate	NADH	NAD+
Control	806 ± 83	193 ± 47	94.4 ± 9.0	4430 ± 980	96 ± 15	280 ± 77
nZnO	931 ± 20	165 ± 38	150 ± 34	4220 ± 750	97 ± 13	216 ± 22

both control and nZnO treated white suckers but there were no significant differences in the magnitude of change between treatments. In control fish, f_v increased by ~55% following atropine injection ($p = 0.042$) while no such increase was noted in nZnO-exposed fish. We also examined AChE activity in brain, heart, and gill tissue to determine if nZnO exposure may trigger ACh accumulation by inhibiting breakdown of the neurotransmitter. There were no differences between treatment groups in either brain or gill tissue, but AChE activity decreased significantly in heart tissue of nZnO treated fish ($p = 0.034$).

3.3. Experiment 2: anaerobic metabolism in white muscle

Previous studies on white sucker indicated that exposure to nZnO may impair aerobic energy metabolism (Bessemer et al., 2015; Dieni et al., 2014). White muscle LDH kinetics were assessed to investigate a potential shift to anaerobic metabolism in fish exposed to 1.0 mg L^{-1} nZnO for 30 h (Table 1). At pH 7.2, the V_{max} in either reaction direction (pyruvate producing or consuming) was unchanged in nZnO treated fish, and no significant differences in the Michaelis constants (K_m) were noted for any substrate. The pH sensitivity of V_{max} was similarly unchanged in fish exposed to nZnO (see Fig. 5).

3.4. Experiment 3: whole animal performance

Fig. 3 details data on O_2 consumption parameters of fish exposed to 1.0 mg L^{-1} nZnO or control conditions. Fish exposed to nZnO exhibited a modest, but significant decrease in MO_{2max} ($p = 0.002$) following the exhaustive chase protocol. A consistent, but non-significant decrease in MO_{2rest} was also noted in nZnO treated fish, which agrees with our previous findings (Bessemer et al., 2015). Aerobic scope was significantly lower ($p = 0.016$) in fish exposed to nZnO, suggesting that nZnO toxicity at the biochemical and cellular level is substantial enough to impair whole animal performance.

Scanning electron microscopy was employed to examine gill filaments for evidence of remodeling and/or damage after exposure to 1.0 mg L^{-1} nZnO. Fig. 4 provides examples of ionocytes, apical pits, mucous globules, and mucous cells as well as quantifications of their occurrence in the filament epithelium. The nZnO-exposed filaments exhibited approximately two times the frequency of apical pits ($p = 0.024$), and c.a. 340% more mucous cells ($p = 0.0048$), with only roughly one half of the surface ($p = 0.042$) ionocytes shown in the control. nZnO-exposed gills also seemed to have much higher mucous coverage, although it was not possible to quantify and may have been an artefact of preparation. There was no clear evidence of an ILCM in either sham-treated fish or nZnO-naïve individuals sampled directly from the holding tank. There was no clear visual evidence of nZnO accumulation on the filaments.

4. Discussion

In two previous studies, our group has examined the mechanisms underlying nZnO toxicity in the white sucker. We showed evidence of oxidative stress in liver (Dieni et al., 2014) and gill (Bessemer et al., 2015) of fish exposed to nZnO. In the current study, there was no evidence of zinc accumulation in any tissue tested after a similar duration of exposure to an even higher dose of nZnO (10 mg L^{-1} vs 1.0 mg L^{-1}). Our previous findings strongly suggested nZnO-mediated gill damage, a temporary bradycardia, and a potentially lowered resting metabolic rate (Bessemer et al., 2015). The purpose of this study was to elucidate the mechanism(s) underlying nZnO toxicity and determine the ecophysiological relevance of the toxic response.

In our previous study, we observed a bradycardia of approximately 35% with nZnO treatment, which resolved by 25 h post-exposure (Bessemer et al., 2015). We were unable to replicate that finding in this study, likely because of the more intensive surgical protocol which extended the duration of anesthesia and potentiated the stress response, as evidenced by the increase in resting f_h. It is also possible that it relates to a hormetic effect of nZnO, as animals here were exposed to a higher concentration of nZnO than in the past (10 mg L^{-1} vs 1.0 mg L^{-1} nZnO). Ventilation rate was significantly higher in fish exposed to 10 mg L^{-1} nZnO for 5 h compared to controls, and treatment with the muscarinic ACh receptor blocker atropine failed to induce a further increase in f_v (Fig. 1). These observations suggest changes in parasympathetic signaling, and support previous findings that nZnO exposure triggers a physiological stress response in white suckers (Bessemer et al., 2015). The depression of AChE activity in heart may also contribute to the observed changes in cardiorespiratory function in nZnO-exposed white suckers. Reducing the rate of enzymatic degradation would lead to accumulation of ACh which would stimulate

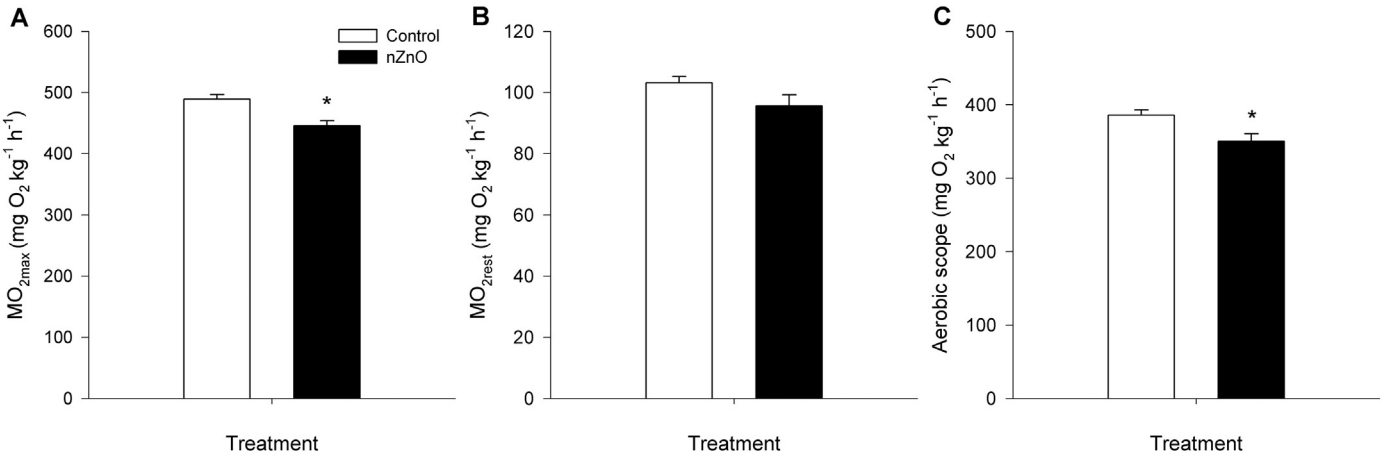

Fig. 3. A, maximum rate of oxygen consumption (MO_{2max}), B, resting rate of oxygen consumption (MO_{2rest}), and C, aerobic scope of white suckers (N = 7 both treatments) exposed to a sham or 1 mg L^{-1} nZnO exposure. Data is presented as mean ± SEM. Asterisks denote a significant difference between treatments ($p < 0.05$).

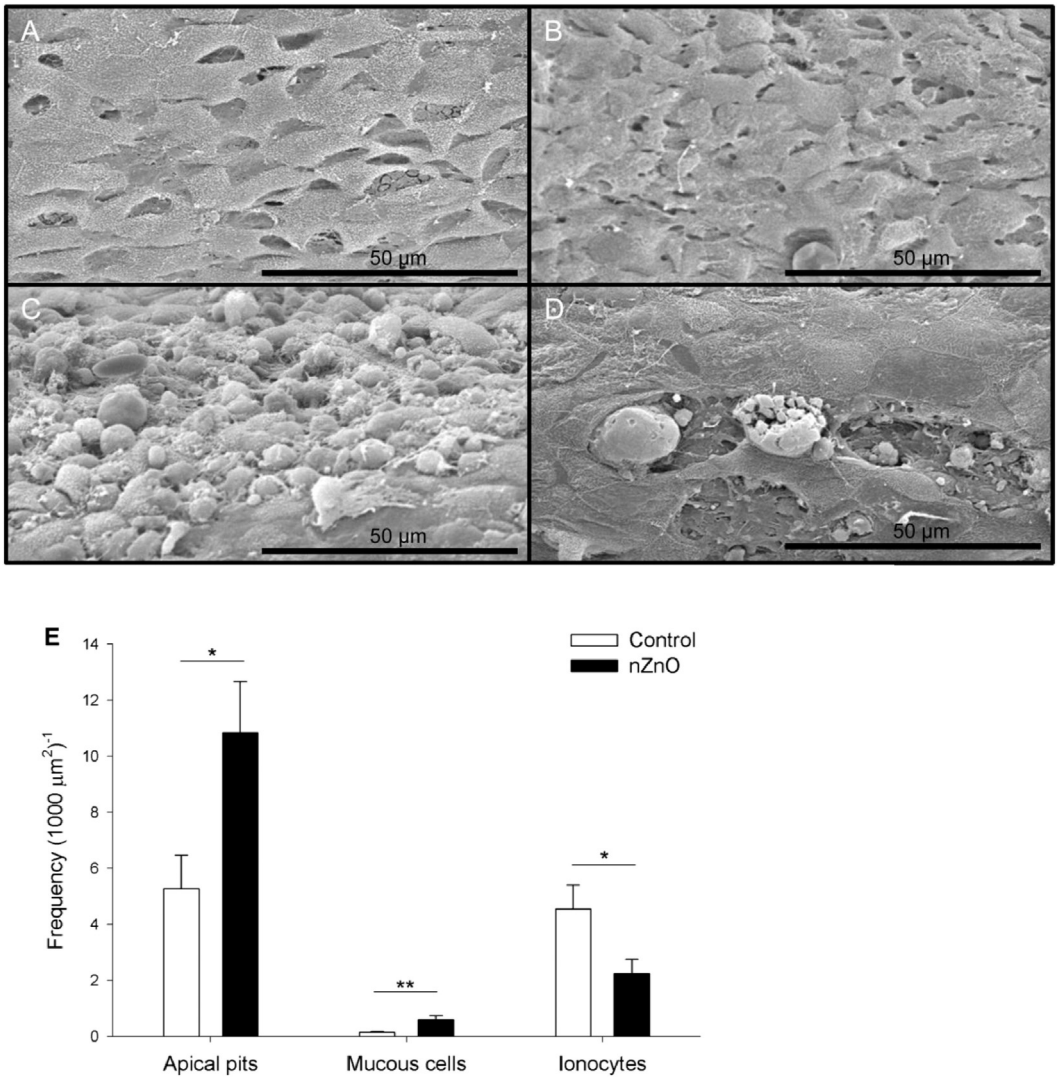

Fig. 4. Scanning electron micrographs of representative gill filaments from fish exposed to a sham (A) or 1 mg L^{-1} nZnO suspension (B-D), all at 500× magnification. Images show examples of ionocytes between pavement cells (A), apical pits (B), mucous globules (C), and mucous cells (D). Scale bars represent 50 μm. Frequency of occurrence of apical pits, mucous cells and ionocytes in the epithelium of the primary gill arch filament (E) (N = 8 both treatments). Data is presented as mean ± SEM. Asterisks denote a significant difference between treatments (*$p < 0.05$, **$p < 0.01$).

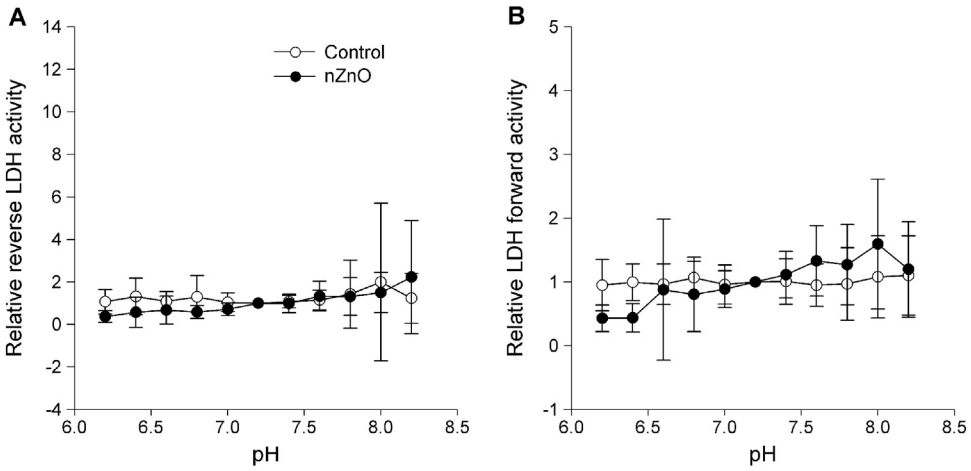

Fig. 5. Maximal rates of white muscle lactate dehydrogenase activity in the lactate-producing (A) and pyruvate-producing (B) reaction directions across a pH range. Fish (N = 10 both treatments) were exposed to either a sham treatment or 1.0 mg L^{-1} suspension of nZnO. Data is presented as activity relative to pH 7.2 for forward (pyruvate-consuming) and reverse (pyruvate-producing) directions. No significant effect of pH was observed between treatments.

inhibitory muscarinic ACh receptors and slow f_h. Blood AChE activity was not assessed but some ENM formulations can inhibit erythrocyte AChE activity in fish (Katuli et al., 2014). The available data support the possibility that damage to the gill epithelium could trigger a pseudo hypoxic response in nZnO-exposed fish, although further studies on gill NEC function are necessary to confirm this interpretation. Given that glycogen stores, plasma lactate levels (Bessemer et al., 2015), and muscle LDH kinetic parameters (current study) do not change with nZnO exposure, it is unlikely that these animals are actually encountering hypoxia or hypoxemia.

Exposure to nZnO tends to decrease MO_{2rest} in nZnO-treated white suckers (Bessemer et al., 2015) and we observed a similar (though not statistically significant) trend in the current study. We also found that exposure to 1.0 mg L^{-1} nZnO significantly depressed MO_{2max}, and to a greater degree than MO_{2rest}. This in turn lead to a significant reduction in aerobic scope, suggesting that nZnO exposure impairs physiological performance in white suckers. A reduction in aerobic scope means that the fish have less energy available to devote to normal processes such as foraging, reproduction, or predator avoidance. Although the absolute reduction in aerobic scope was small (9%), the exposure duration was quite short, so it is possible that such effects would be magnified in a more environmentally relevant chronic exposure situation. Changes in gill morphology (see below) and the regulation of f_h associated with nZnO exposure may restrict O_2 uptake and delivery, explaining the observed depression of MO_{2max}.

The halving of ionocyte incidence on the gill filament epithelium co-occurred with a doubling of apical pit density. We previously observed activation of apoptotic markers in nZnO-exposed gill tissue, including increases in caspase activity and heat shock protein expression (Bessemer et al., 2015). Apical pits provide increased surface area and show high NKA expression (Christensen et al., 2012), supporting our previous finding of increased NKA activity in the gill tissue of nZnO-exposed fish. These findings suggest that the loss of ionoregulatory surface area due to ionocyte apoptosis may be mitigated by the formation of NKA-rich apical pits. The increase in mucous cell incidence is likely in response to irritation of the epithelium as has been seen in other fish species exposed to ENMs (Federici et al., 2007; Smith et al., 2007). Damage to the gill epithelium in nZnO exposed white suckers also induces increased Na^+/K^+-ATPase activity, ostensibly to maintain plasma osmolality (Bessemer et al., 2015).

5. Conclusions

This study aimed to elucidate the biological importance of nZnO toxicity in freshwater fish and to characterize mechanisms of bioactivity. We specifically focused on whether gill damage associated with ENM exposure could influence the regulation of cardiorespiratory function and subsequently impact aerobic capacity in the whole animal. Our findings suggest that even in the absence of detectable nZnO or free Zn^{2+} accumulation, gill damage and changes in ACh metabolism reduced maximal O_2 uptake capacity in white suckers and trigger cardiorespiratory changes. Acute, short term exposure to nZnO also significantly reduced whole animal aerobic scope. The observed reductions in MO_{2max} and aerobic scope were modest, but raise concerns regarding the potential physiological impacts of chronic nZnO exposure in wild fish. Long term, environmentally relevant nZnO exposure studies incorporating behavioral and reproductive metrics would be valuable in determining the potential ecological implications of the findings presented here.

Acknowledgements

This study was funded by a Natural Science and Engineering Research Council of Canada (NSERC) Discovery (418238) and New Brunswick Health Research Foundation (490) operating grants to TJM, and a Mount Allison University President's Creative Research Award to CAD. NIC was supported by a Goodridge Undergraduate Research Award, an NSERC Canada Graduate Scholarship-Master's, and a New Brunswick Innovation Fund scholarship. GJPA was supported by a Carnegie undergraduate research scholarship and TER by an R.P. Chapman Award from Mount Allison University. CAD was the Mount Allison University Margaret and Wallace McCain Postdoctoral Fellow and recipient of a Mount Allison University President's Research and Creative Activities Fund operating grant. The authors would like to thank Mr. James Ehrman for his assistance with SEM studies, and Mr. Wayne Anderson for animal acquisition and care.

References

Bai, W., Zhang, Z., Tian, W., He, X., Ma, Y., Zhao, Y., Chai, Z., 2010. Toxicity of zinc oxide nanoparticles to zebrafish embyo: a physiochemical study of toxicity mechanism. J. Nanopart. Res. 12, 1645–1654.

Bessemer, R.A., Butler, K.M.A., Tunnah, L., Callaghan, N.I., Rundle, A., Currie, S., Dieni, C.A., MacCormack, T.J., 2015. Cardiorespiratory toxicity of environmentally relevant zinc oxide nanoparticles in the freshwater fish *Catostomus commersonii*. Nanotoxicology 9, 861–870. http://dx.doi.org/10.3109/17435390.2014.982737.

Bilberg, K., Malte, H., Wang, T., Baatrup, E., 2010. Silver nanoparticles and silver nitrate cause respiratory stress in Eurasian perch (*Perca fluviatilis*). Aquat. Toxicol. 96, 159–165.

Christensen, A.K., Hiroi, J., Schultz, E.T., McCormick, S.D., 2012. Branchial ionocyte organization and ion-transport protein expression in juvenile alewives acclimated to freshwater or seawater. J. Exp. Biol. 215, 642–652. http://dx.doi.org/10.1242/jeb.063057.

Danovaro, R., Bongiorni, L., Corinaldesi, C., Giovannelli, D., Damiani, E., Astolfi, P., Greci, L., Pusceddu, A., 2008. Sunscreens cause coral bleaching by promoting viral infections. Environ. Health Perspect. 116, 441–447.

Dieni, C., Stone, C., Armstrong, M., Callaghan, N., MacCormack, T., 2013. Spherical gold nanoparticles impede the function of bovine serum albumin in vitro: a new consideration for studies in nanotoxicology. J. Nanomater. Mol. Nanotechnol. 2. http://dx.doi.org/10.4172/2324-8777.1000124.

Dieni, C.A., Callaghan, N.I., Gormley, P.T., Butler, K.M.A., Maccormack, T.J., 2014. Physiological hepatic response to zinc oxide nanoparticle exposure in the white sucker, *Catostomus commersonii*. Comp. Biochem. Physiol., Part C: Toxicol. Pharmacol. 162, 51–61. http://dx.doi.org/10.1016/j.cbpc.2014.03.009.

Dymowska, A.K., Hwang, P.P., Goss, G.G., 2012. Structure and function of ionocytes in the freshwater fish gill. Respir. Physiol. Neurobiol. 184, 282–292. http://dx.doi.org/10.1016/j.resp.2012.08.025.

Evans, D., Piermarini, P., Choe, K., 2005. The multifunctional fish gill: dominant site of gas exchange, osmoregulation, acid-base regulation, and excretion of nitrogenous waste. Physiol. Rev. 85, 97–177.

Federici, G., Shaw, B., Handy, R., 2007. Toxicity of titanium dioxide nanoparticles to rainbow trout (*Oncorhynchus mykiss*): gill injury, oxidative stress, and other physiological effects. Aquat. Toxicol. 84, 415–430.

Gimbert, L.J., Hamon, R.E., Casey, P.S., Worsfold, P.J., 2007. Partitioning and stability of engineered ZnO nanoparticles in soil suspensions using flow field-flow fractionation. Environ. Chem.

Guo, D., Bi, H., Liu, B., Wu, Q., Wang, D., Cui, Y., 2013. Reactive oxygen species-induced cytotoxic effects of zinc oxide nanoparticles in rat retinal ganglion cells. Toxicol. In Vitro 27, 731–738.

Hao, L., Chen, L., 2012. Oxidative stress responses in different organs of carp (*Cyprinus carpio*) with exposure to ZnO nanoparticles. Ecotoxicol. Environ. Saf. 80, 103–110. http://dx.doi.org/10.1016/j.ecoenv.2012.02.017.

Katuli, K.K., Massarsky, A., Hadadi, A., Pourmehran, Z., 2014. Silver nanoparticles inhibit the gill Na+/K+-ATPase and erythrocyte AChE activities and induce the stress response in adult zebrafish (*Danio rerio*). Ecotoxicol. Environ. Saf. 106, 173–180. http://dx.doi.org/10.1016/j.ecoenv.2014.04.001.

Liu, L., Wang, X., Yang, X., Fan, W., Wang, X., Wang, N., Li, X., Xue, F., 2014. Preparation, characterization, and biotoxicity of nanosized doped ZnO photocatalyst. Int. J. Photoenergy.

MacCormack, T.J., Clark, R.J., Dang, M.K.M., Ma, G., Kelly, J.A., Veinot, J.G.C., Goss, G.G., 2012. Inhibition of enzyme activity by nanomaterials: potential mechanisms and implications for nanotoxicity testing. Nanotoxicology 6, 515–525.

Milsom, W., Burleson, M., 2007. Peripheral arterial chemoreceptors and the evolution of the carotid body. Respir. Physiol. Neurobiol. 157, 4–11.

Ong, K.J., MacCormack, T.J., Clark, R.J., Ede, J.D., Ortega, V.a., Felix, L.C., Dang, M.K.M., Ma, G., Fenniri, H., Veinot, J.G.C., Goss, G.G., 2014. Widespread nanoparticle-assay interference: implications for nanotoxicity testing. PLoS One 9. http://dx.doi.org/10.1371/journal.pone.0090650.

Perry, S.F., Desforges, P., 2006. Does bradycardia or hypertension enhance gas transfer in rainbow trout (*Oncorhynchus mykiss*). Comp. Biochem. Physiol., Part A 144, 163–172.

Piccino, F., Gottschalk, F., Seeger, S., Nowack, B., 2012. Industrial production quantities and uses of ten engineered nanomaterials in Europe and the world. J. Nanopart. Res. 14.

Regan, K., Jonz, M., Wright, P., 2011. Neuroepithelial cells and the hypoxia emersion response in the amphibious fish *Kryptolebias marmoratus*. J. Exp. Biol. 214, 2560–2568.

Reidy, S., Nelson, J., Tang, Y., Kerr, S., 1995. Post-exercise metabolic rate in Atlantic cod and its dependence upon the method of exhaustion. J. Fish Biol. 47, 377–386.

Schultz, A.G., Ong, K.J., Maccormack, T., Ma, G., Veinot, J.G.C., Goss, G.G., 2012. Silver Nanoparticles Inhibit Sodium Uptake in Juvenile Rainbow Trout (*Oncorhynchus mykiss*). 46 pp. 10295–10301.

Sharma, V., Singh, P., Pandey, A., Dhawan, A., 2012. Induction of oxidative stress, DNA damage and apoptosis in mouse liver after sub-acute oral exposure to zinc oxide nanoparticles. Mutat. Res. 745, 84–91.

Smith, C., Shaw, B., Handy, R., 2007. Toxicity of single walled carbon nanotubes to rainbow trout, (*Oncorhynchus mykiss*): respiratory toxicity, organ pathologies, and other physiological effects. Aquat. Toxicol. 82, 94–109.

Sollid, J., Nilsson, G.E., 2006. Plasticity of respiratory structures - adaptive remodeling of fish gills induced by ambient oxygen and temperature. Respir. Physiol. Neurobiol. 154, 241–251. http://dx.doi.org/10.1016/j.resp.2006.02.006.

Song, W., Zhang, J., Guo, J., Zhang, J., Ding, F., Li, L., Sun, Z., 2010. Role of the dissolved zinc ion and reactive oxygen species in cytotoxicity of ZnO nanoparticles. Toxicol. Lett. 193, 389–397.

Soofiani, N.M., Priede, I.G., 1985. Aerobic metabolic scope and swimming performance in juvenile cod, *Gadus morhua* L. J. Fish Biol. 26, 127–138.

Tano de la Hoz, M.F., Longo, M.V., Escalante, A.H., Diaz, A.O., 2014. Surface ultrastructure of the gills of *Odontesthes bonariensis* (Valenciennes, 1835) (Teleostei: Atheriniformes) from a temperate shallow lake. Int. J. Morphol. 32, 1341–1346.

Taylor, E., Leite, C., Florindo, L., Belao, T., Rantin, F., 2009. The basis of vagal efferent control of heart rate in a neotropical fish, the pacu, *Piaractus mesopotamicus*. J. Exp. Biol. 212, 906–913.

Wong, S., Leung, P., Djurisic, A., Leung, K., 2010. Toxicities of nano zinc oxide to five marine organisms: influences of aggregate size and ion solubility. Anal. Bioanal. Chem. 396, 609–618.

Xia, T., Kovochich, M., Liong, M., Madler, L., Gilbert, B., Shi, H., Nel, A., 2008. Comparison of the mechanism of toxicity of zinc oxide and cerium oxide nanoparticles based on dissolution and oxidative stress properties. ACS Nano 2, 2121–2134.

Xiong, D., Fang, T., Yu, L., Sima, X., Zhu, W., 2011. Effects of nano-scale TiO2, ZnO and their bulk counterparts on zebrafish: acute toxicity, oxidative stress and oxidative damage. Sci. Total Environ. 409, 1444–1452.

Yu, T., Fang, D., Xiong, D., Zhu, W., Sima, X., 2011. Comparative toxicity of nano-ZnO and bulk ZnO suspensions to zebrafish and the effects of sedimentation, radical OH production and particle dissolution in distilled water. J. Environ. Monit. 13, 1975–1982.

Zhu, X., Zhu, L., Duan, Z., Qi, R., Li, Y., Lang, Y., 2008. Comparative toxicity of several metal oxide nanoparticle aqueous suspensions to zebrafish (*Danio rerio*) early developmental stage. J. Environ. Sci. Health., Part A 43, 278–281. http://dx.doi.org/10.1080/10934520701792779.

Zhu, X., Wang, J., Zhang, X., Chang, Y., Chen, Y., 2009. The impact of ZnO nanoparticle aggregates on the embryonic development of zebrafish (*Danio rerio*). Nanotechnology 20, 195103. http://dx.doi.org/10.1088/0957-4484/20/19/195103.